Revista Mexicana de Astronomía y Astrofísica
Universidad Nacional Autónoma de México
rmaa@astroscu.unam.mx
ISSN (Versión impresa): 0185-1101
MÉXICO

2008
Yair Krongold / Fabrizio Nicastro / Martin Elvis / Nancy Brickhouse / Elena Jiménez Bailón / Luc Binette / Smita Mathur
CAN IONIZED OUTFLOWS IN AGN PRODUCE IMPORTANT FEEDBACK EFFECTS? THE CASE OF NGC 4051
Revista Mexicana de Astronomía y Astrofísica, abril, volumen 032
Universidad Nacional Autónoma de México
Distrito Federal, México
pp. 123-127

RevMexAA (Serie de Conferencias), **32**, 123–127 (2008)

CAN IONIZED OUTFLOWS IN AGN PRODUCE IMPORTANT FEEDBACK EFFECTS? THE CASE OF NGC 4051

Yair Krongold,[1] Fabrizio Nicastro,[2,3] Martin Elvis,[3] Nancy Brickhouse,[3] Elena Jiménez-Bailón,[1] Luc Binette,[1] and Smita Mathur[4]

RESUMEN

Usando una observación de 100 ks del satélite XMM-Newton de la galaxia Seyfert 1 de Líneas Delgadas NGC 4051, mostramos que es posible medir todos los parámetros físicos del viento ionizado en un Núcleo Activo siguiendo la respuesta del estado de ionización de los absorbedores de rayos-X a cambios del continuo ionizante. Encontramos que el orígen más plausible para el viento es el disco de acreción. Un flujo radial no es favorecido, indicando que la geometría del viento debe ser similar a la de un cono. La tasa de transporte de masa del viento resultó del $2-5\%$ de la tasa de acreción. Si este radio es representativo de todos los Núcleos Activos, entonces aún los cuásares más luminosos serían incapaces de tener algún efecto importante en su medio ambiente a gran escala, a menos que los vientos estén siendo observados antes de ser acelerados. Sólo en un escenario como éste, los vientos ionizados en Núcleos Activos de Galaxias podrían producir una retroalimentación a nivel cósmico.

ABSTRACT

Using a 100 ks XMM-Newton exposure of the Narrow Line Seyfert 1 NGC 4051, we show that the time evolution of the ionization state of the X-ray absorbers in response to the rapid and highly variable X-ray continuum constrains all the main physical and geometrical properties of an AGN *Warm Absorber* wind. An accretion disk origin for the warm absorber wind is strongly suggested. A radial flow in a spherical geometry is unlikely, and a conical wind geometry is preferred. The implied mass outflow rate from this wind, can be well constrained, and is $2-5$ % of the mass accretion rate. If the mass outflow rate scaling with accretion rate is representative of all quasars, our results imply that warm absorbers in powerful quasars are unlikely to produce important evolutionary effects on their larger environment, unless we are observing the winds before they get fully accelerated. Only in such a scenario can AGN winds be important for cosmic feedback.

Key Words: galaxies: absorption lines — galaxies: active — galaxies: Seyfert — X-rays: galaxies

1. IONIZED WINDS IN AGN

Ionized absorption winds (*Warm Absorbers*: WA) are observed in the Ultraviolet (UV) and X-ray spectra of ≥ 50 % of Seyfert 1s (e.g. Crenshaw et al. 2003) and quasars (Piconcelli et al. 2005), with line of sight velocities of the order of a few hundreds to ~ 2000 km s^{-1}. Such high detection rates, combined with evidence for transverse flows (Mathur et al. 1995; Crenshaw et al. 2003) suggest that WAs are actually ubiquitous in AGN, but become directly visible in absorption only when our line of sight crosses the outflowing material. Despite their ubiquity, very little is still known about their physical state, dynamical strength and geometry.

[1]Instituto de Astronomía, Universidad Nacional Autónoma de México, Apdo. Postal 70-264, 04510 México, D. F., México (yair@astroscu.unam.mx).

[2]Osservatorio Astronomico di Roma-INAF, Rome, Italy.

[3]Harvard-Smithsonian Center for Astrophysics, 60 Garden Street, Cambridge, MA 02138, USA.

[4]Ohio State University, 140 West 18th Avenue, Columbus, OH 43210, USA.

The most fundamental question is where do quasar winds originate? Proposals span a factor $> 10^6$ in radius and include (a) the Narrow Line Region (Kinkhabwala et al. 2002; Ogle et al. 2004), (b) the inner edge of the 'obscuring torus' (Krolik & Kriss 2001), and (c) the accretion disk itself (Elvis 2000). Discriminating among these widely different scales (~ 10 kpc to ~ 0.001 pc) requires the independent determination of a quantity which is not directly observable: the electron density n_e of the outflowing material, which then gives the distance R from the central ionizing source.

2. THE IMPORTANCE OF TIME-EVOLVING PHOTOIONIZATION

Recent efforts to understand WAs have concentrated on modeling the time-averaged, high signal-to-noise (S/N), high-resolution X-ray spectra of nearby Seyferts (e.g. Krongold et al. 2003; Netzer et al. 2003, Krongold et al. 2005a). These studies have shown that there are just a few distinct phys-

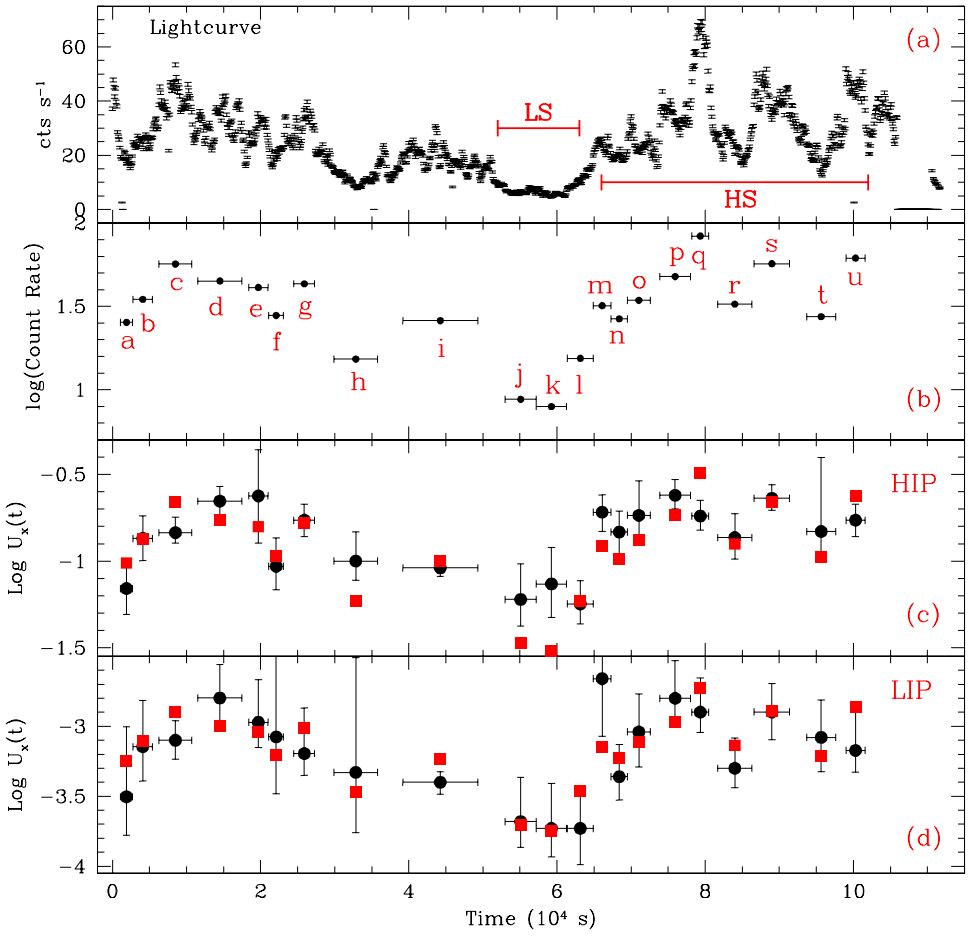

Fig. 1. Panel (a): Lightcurve of NGC 4051 in bins of 100 s. Panel (b): Log of the count rate vs. time, for the 21 "flux states" used to study the variability of the warm absorber. Spectra were extracted for each of the 21 bins, with an exposure time given by the x error bars. Panel (c) and (d): Ionization parameter of the HIP (c) and LIP (d) as a function of time. The red squares represent the expected value of U_x if the gas were in photoionization equilibrium with the continuum source.

ical components in these outflows. However, only average estimates of the product $(n_e R^2)$ could be derived for each component, due to the intrinsic degeneracy of n_e and R in the equation that defines the two observables: the average ionization parameter of the gas $U_x = Q_x/(4\pi R^2 c n_e)$ and the luminosity of ionizing photons Q_x.

By monitoring the response of the ionization state of the gas in the wind to changes of the ionizing continuum, it is possible to measure the density n_e of the gas (Krolik & Kriss 1995; Nicastro et al. 1999). Hence, time-evolving photoionization gives an unambiguous method to remove this degeneracy and measure the distance R of the wind from the ionizing source. The diagnostic power of this method relies in the fact that the *photoionization equilibrium timescale* (i.e. the time necessary for the gas to reach photoionization equilibrium with the ionizing source) t_{eq} depends explicitely in the electron density n_e of the absorbing gas.

Here, we apply this technique to a XMM-Newton observation of the variable Seyfert 1 galaxy NGC 4051, to effectively track changes in the WA properties over small time scales.

3. THE IONIZED OUTFLOW IN NGC 4051

NGC 4051 was observed for ∼117 ks with the XMM-Newton Observatory, on 2001 May 16–17 (Obs. Id. 0109141401). The source varied by a factor of a few on timescales as short as 1 ks, and by a factor of ∼ 12 from minimum to maximum flux over the whole observation (see Figure 1a). Full details

of the data reduction and analysis can be found in Krongold et al. (2007, hereafter K07).

Two physically distinct, but dinamically coincident ($v_{out} \sim 500$ km s^{-1}), ionization components were present in the RGS spectrum of the whole observation: a high-ionization phase (HIP) and a low-ionization phase (LIP).

4. FOLLOWING THE TIME-VARIABILITY OF THE IONIZED ABSORBERS IN NGC 4051

To study the response of the WAs of NGC 4051 to ionizing flux changes, we performed a time-resolved analysis of the EPIC-PN data. Since NGC 4051 varies on typical timescales of only a few ks, the best constraints on the time dependence of the ionized absorbers will come from spectra in time bins of similar duration. Our aim was to detect and constrain possible variations in the opacity of the ionized absorbers (detecting changes in U_X) on timescales as short as few ks. We extracted and analized EPIC-PN spectra from 21 distinct continuum levels (*a*-*u*, see Figure 1b).

For both absorbing components the derived U_X values follow closely the source continuum lightcurve [compare panel (c) and (d) with panel (b) of Figure 1], clearly indicating that the gas is responding quickly to the changes in the ionizing continuum.

To study more quantitatively how these changes are related to the changes in the continuum, we show in Figure 2a,b the log of the source count rate (log $C(t)$) vs. log $U_X(t)$, for the HIP [panel (a)] and the LIP [panel (b)]. For most of the points of the HIP and for all the points of the LIP (within 2σ), log $C(t)$ correlates with log $U_X(t)$ tightly, which allow us to derive robust estimates of the quantity ($n_e R^2$) (best fit lines in Figure 2).

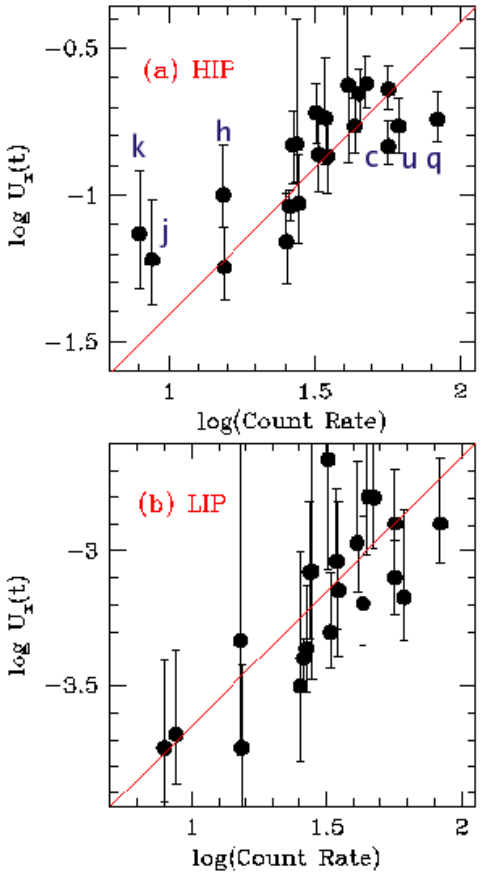

Fig. 2. Log $U_X(t)$ vs. log of the source count rate (log $C(t)$), for the HIP [panel (a)] and the LIP [panel (b)]. For most of the points of the HIP and for all points of the LIP, log $C(t)$ correlates with log $U_X(t)$ tightly. HIP and LIP are close to photoionization equilibrium. The solid lines represents the photoionization equilibrium relation and determine the values of $n_e R^2$ for the two components.

5. THE IONIZED ABSORBER IN NGC 4051: A DENSE, COMPACT DISK WIND

5.1. *Physical conditions, Location and Structure*

Since all the points for the LIP are consistent with photoionization equilibrium within 2σ (Figure 2b), the LIP can both recombine and ionize in a timescale shorter than the shortest time interval separating spectra with large flux changes. Thus, we conclude that the *photoionization equilibrium timescale* $t_{eq}(LIP) < 3$ ks. The response time of the gas to changes in the continuum set strong constraints on the density, n_e, and location, R, of the absorber relative to the continuum source (see Krongold et al. 2005b and K07 for details). For the LIP we find $n_e(LIP) > 8.1\times10^7$ cm^{-3} and $R_{LIP} <$ 3.5 light-days (see Table 1).

For the HIP, the situation is somewhat more complicated. The spectra of the HIP at typical count-rates are all consistent with photoionization equilibrium. The extreme flux points, on the other hand, show deviations from equilibrium, i.e. they fail to respond as expected to the changes in the continuum. This behavior is expected in gas close to, but not instantaneously in, equilibrium with the ionizing flux, since, depending on gas density, a cloud can respond quickly (few ks) to smooth and moderate increases/decreases of the ionizing continuum, but would require longer times to respond to fast and extreme flux changes (Nicastro et al. 1999). Unlike the LIP (for which only an upper limit on t_{eq} can be estimated), the behavior of the HIP allows us to set both lower and upper limits on $t_{eq}(HIP)$. We find

TABLE 1

PHYSICAL PARAMETERS OF HIGH AND LOW IONIZATION ABSORBERS

Abs.	N_H 10^{21} cm^{-2}	T_e 10^5 K	$(n_e R^2)$ 10^{38} cm^{-1}	n_e 10^7 cm^{-3}	P_e 10^{12} K cm^{-3}	R 10^{15} cm	ΔR 10^{14} cm	$(\Delta R/R)$
HIP	(3.2 ± 2.2)	(5.4 ± 1.4)	(0.38 ± 0.05)	(0.58–2.1)	(2.9–10.5)	(1.3–2.6)	(1.9–7.2)	(0.1–0.2)
LIP	(0.59 ± 0.28)	$(0.28 \pm .04)$	(66 ± 3)	> 8.1	> 2.4	< 8.9	< 0.09	$< 10^{-3}$

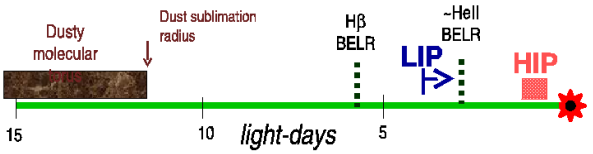

Fig. 3. Location of features in the nuclear environment of NGC 4051 on a light-day scale.

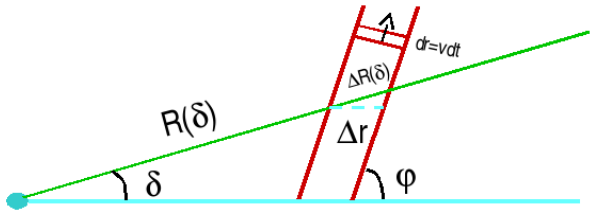

Fig. 4. Disk-Wind in a conical geometry. ϕ is the angle formed by the wind and the disk and δ the angle between the disk and the observer's line of sight. R is the distance from the continuum source to the wind and ΔR its thickness.

$t_{eq}(HIP) \sim 3 - 10$ ks, which implies $n_e(HIP) = (5.8 - 21.0) \times 10^6$ cm^{-3} and $R_{HIP} = 0.5 - 1.0$ light-days (Table 1).

The observed variability of the gas also sets constraints on the structure of the ionized absorber. Assuming homogeneity in the flow, and using the column densities and number densities inferred in our analysis, the line of sight thickness and relative thickness of the wind can be estimated. For our two components, we find $\Delta R_{LIP} < 9 \times 10^{12}$ cm, $\Delta R_{HIP} = (1.9 - 7.2) \times 10^{14}$ cm, and $(\Delta R/R)_{LIP} < 10^{-3}$ and $(\Delta R/R)_{HIP} = (0.1 - 0.2)$ (Table 1).

5.2. *The Accretion-Disk Origin of the Ionized Wind*

The location of the HIP in Schwarzschild radii (R_s) implies that the origin of the HIP is related to the accretion disk. In these units, R_{HIP}= 2300–4600 R_s, which locates the outflow in the outer regions of the accretion disk, but at distances shorter than the radius where an α-disk becomes gravitationally unstable ($\sim$ 35000 R_s; Goodman 2003). The LIP is also likely related to the disk, as $R_{LIP} < 15800 R_s$. Figure 3 gives a scale diagram of the location of the different AGN components.

5.3. *Geometry of the Wind*

Our findings considered alone, are consistent with thin spherical shells of material which are expelled radially from the central ionizing source. However, we consider this configuration implausible because of the fine tuning required in the frequency with which these shells of material would have to be produced to explain the high occurrence of WAs in AGN, and yet still avoid having the thin shells degenerate into a continuous flow (which is strictly ruled out for NGC 4051). The next simplest geometrical configuration is that of a bi-conical wind (Figure 4; Elvis 2000). All our estimates for the physical and geometrical quantities of the two X-ray absorbers of NGC 4051 are consistent with this scenario, and recent magneto-hydrodynamical simulations also favor this interpretation (Everett 2005).

5.4. *Wind Mass Outflow Rate*

With the location and density of the X-ray absorbing material in hand, and assuming the above bi-conical geometry, we can now estimate the mass outflow rate of the wind using the observables v_r (the line of sight outflow velocity), N_H (the line of sight equivalent H column density), and R (see K07 for full details).

For a vertical disk wind (Figure 4) we find: $\dot{M}_w(HIP) = (0.7 - 1.4) \times 10^{-4} M_\odot$ yr^{-1} and $\dot{M}_w(LIP) < 0.9 \times 10^{-4} M_\odot$ yr^{-1}. For NGC 4051, assuming 10% accretion efficiency, the observed accretion rate is $\dot{M}_{accr} = 4.7 \times 10^{-3} M_\odot$ yr^{-1} (Peterson et al. 2004), so $\dot{M}_w(HIP) = (0.02 - 0.03)\dot{M}_{accr}$ and $\dot{M}_w(LIP) < 0.02\dot{M}_{accr}$. Therefore, the total mass outflow rate from the LIP and the HIP, in NGC 4051, is $\dot{M}_{out} = (0.02 - 0.05)\dot{M}_{accr}$.

6. POSSIBLE IMPLICATIONS FOR GALAXY EVOLUTION AND COSMIC FEEDBACK

Assuming that the black hole mass of NGC 4051 was all accreted ($M_{BH} = 1.9 \times 10^6 M_\odot$, Peterson et

al. 2004), we can calculate the integrated lifetime mass lost due to the X-ray winds, $M_{out} = (0.4 - 1.0) \times 10^5 M_\odot$. If the measured ratio $\dot{M}_{out}/\dot{M}_{accr}$ of NGC 4051 is representative of the quasar population, then for winds in powerful quasars ($L_{bol} \sim 10^{47}$ erg s^{-1}, M_{BH} = few$\times 10^9$ $M_\odot$) the total mass outflow could be as large as $M_{out} \sim$ few$\times 10^8$ $M_\odot$ (neglecting any additional mass from the interstellar medium entrained in the wind). This mass could, in principle, be deployed into the IGM surrounding the quasar's host galaxy. As the quasar nuclear environment is unusually rich in metals (Hamman & Ferland 1999; Fields et al. 2005, 2007), quasar winds could feed their local IGM with highly metal enriched material. Thus, metal rich IGM systems may be significantly stronger close to powerful quasars.

Simulations show that, if quasar winds are to be the main process controlling the evolution of the host galaxy and the surrounding IGM, they require output kinetic energies of the order of $\sim 10^{60}$ erg (e.g. Hopkins et al. 2005; Scannapieco 2004; King 2003). Such energy outputs would be enough to produce the well known relation between the central black hole mass and bulge velocity dispersion (Ferrarese & Merrit 2000; Gebhardt et al. 2000), or to heat the IGM controlling structure formation.

If the measured ratio $\dot{M}_{out}/\dot{M}_{accr}$ is representative of quasars, then (assuming velocities in our line of sight of 500 km s^{-1}) the total energy deployed by a powerful quasar into the host galaxy ISM or the IGM, during the AGN active phase, could be $\sim few \times 10^{57}$ erg. Thus, winds in powerful quasars would still be too weak to have a drastic influence on the whole galaxy evolution. We note, however, that it is likely that we are not seeing the full terminal velocity of the wind (Proga & Kallman 2004; Elvis 2000). Then, if the winds are accelerated to v$\sim$5000 km s^{-1}, i.e. by a factor of 10 (which is the ratio between the velocities found in WAs and BALQSOs), the total kinetic energy deployed by these systems could reach $\sim$ few$\times 10^{59}$ erg, similar to the binding energy of massive galactic bulges. This energy is comparable to the 10^{60} erg required by simulations for quasar winds to be critically important in feedback processes (e.g. Hopkins et al. 2005; Scannapieco 2004; King 2003).

Thus, despite our low mass loss rate estimates, it still remains possible that AGN winds are important for at least two major feedback mechanisms: (1) the evolution of their host galaxies, putting energy into the ISM of the host and controlling the accretion process, thus regulating the black hole growth (the relationship between the mass of the central black hole in galaxies and the velocity dispersion of the galactic bulge), and/or (2) enriching with metals the IGM and heating this medium, controlling the accretion of material onto galaxies (thus controlling structure formation).

This work was supported by CONACyT grants J-50296 and J-49594.

REFERENCES

Crenshaw, D. M., Kraemer, S. B., & George, I. M. 2003, A&A Rev., 41, 117
Elvis, M. 2000, ApJ, 545, 63
Everett, J. E. 2005, ApJ, 631, 689
Ferrarese, L., & Merritt, D. 2000, ApJ, 539, L9
Fields, D. L., Mathur, S., Pogge, R. W., Nicastro, F., Komossa, S., & Krongold, Y. 2005, ApJ, 634, 928
Fields, D. L., Mathur, S., Krongold, Y., Williams, R., & Nicastro, F. 2007, ApJ, 666, 828
Gebhardt, K., et al. 2000, ApJ, 539, L13
Goodman, J. 2003, MNRAS, 339, 937
Hamann, F., & Ferland, G. 1999, ARA&A, 37, 487
Hopkins, P. F., Hernquist, L., Cox, T. J., Di Matteo, T., Robertson, B., & Springel, V. 2005, ApJS, 163, 1
King, A. 2003, ApJ, 596, L27
Kinkhabwala, A., et al. 2002, ApJ, 575, 732
Krolik, J. H., & Kriss, G. A. 1995, ApJ, 447, 512
_____. 2001, ApJ, 561, 684
Krongold, Y., Nicastro, F., Brickhouse, N. S., Elvis, M., Liedahl, D. A. & Mathur, S. 2003, ApJ, 597, 832
Krongold, Y., Nicastro, F., Elvis, M., Brickhouse, N. S., Mathur, S., & Zezas, A. 2005a, ApJ, 620, 165
Krongold, Y., Nicastro, F., Brickhouse, N. S., Elvis, M., & Mathur, S. 2005b, ApJ, 622, 842
Krongold, Y., Nicastro, F., Elvis, M., Brickhouse, N., Binette, L., Mathur, S., & Jiménez-Bailón, E. 2007, ApJ, 659, 1022 (K07)
Mathur, S., Elvis, M., & Wilkes, B. 1995, ApJ, 452, 230
Netzer, H., et al. 2003, ApJ, 599, 933
Nicastro, F., Fiore, F., & Matt, G. 1999, ApJ, 517, 108
Ogle, P. M., Marshall, H. L., Lee, J. C., & Canizares, C. R. 2000, ApJ, 545, L81
Peterson, B. M., et al. 2004, ApJ, 613, 682
Piconcelli, E., Jimenez-Bailón, E., Guainazzi, M., Schartel, N., Rodríguez-Pascual, P. M., & Santos-Lleó, M. 2005, A&A, 432, 15
Proga, D., & Kallman, T. R. 2004, ApJ, 616, 688
Scannapieco, E., & Oh, S. P. 2004, ApJ, 608, 62